Published in final edited form as:
Bioconjug Chem. 2009 November 18; 20(11): 2177–2184. doi:10.1021/bc900362k.

Dual-modality molecular imaging using antibodies labeled with activatable fluorescence and a radionuclide for specific and quantitative targeted cancer detection

Mikako Ogawa, **Celeste A.S. Regino**, **Jurgen Seidel**, **Michael V. Green**, **Wenze Xi**, **Mark Williams**, **Nobuyuki Kosaka**, **Peter L Choyke**, and **Hisataka Kobayashi**
Molecular Imaging Program, Center for Cancer Research, National Cancer Institute, National Institute of Health

Abstract

Multimodality molecular imaging should have potential for compensating the disadvantages and enhancing the advantages of each modality. Nuclear imaging is superior to optical imaging in whole body imaging and in quantification due to good tissue penetration of gamma rays. However, target specificity can be compromised by high background signal due to the always signal ON feature of nuclear probes. In contrast, optical imaging can be superior in target specific imaging by employing target-specific signal activation systems, although it is not quantitative because of signal attenuation. In this study, to take advantage of the mutual cooperation of each modality, multimodality imaging was performed by a combination of quantitative radiolabeled probe and an activatable optical probe. The monoclonal antibodies, panitumumab (anti-HER1) and trastuzumab (anti-HER2) were labeled with ^{111}In and ICG, and tested in both HER1 and HER2 tumor bearing mice by the cocktail injection of radiolabeled and optical probes, and by the single injection of a dual-labeled probe. The optical and nuclear images were obtained over 6 days after the conjugates injection. The fluorescence activation properties of ICG labeled antibodies were also investigated by *in vitro* microscopy. *In vitro* microscopy demonstrated that there was no fluorescence signal with either panitumumab-ICG or trastuzumab-ICG, when the probes were bound to cell surface antigens but were not yet internalized. After the conjugates were internalized into the cells, both conjugates showed bright fluorescence signal only in the target cells. These results show both conjugates work as activatable probes. *In vivo* multimodality imaging by injection of a cocktail of radio-optical probes, only the target specific tumor was visualized by optical imaging. Meanwhile, the biodistribution profile of the injected antibody was provided by nuclear imaging. Similar results were obtained with radio and optical dual labeled probe, and it is confirmed that pharmacokinetic properties did not affect the results above.

Here, we could characterize the molecular targets by activatable optical probes, and visualize the delivery of targeting molecules quantitatively by radioactive probes. Multimodality molecular imaging combining activatable optical and radioactive probe has great potential for simultaneous visualization, characterization, and measurement of biological processes.

INTRODUCTION

To date, *in vivo* molecular imaging techniques have made great progress due to improvements in imaging technology and the design of novel imaging probes. Several modalities are now

Corresponding Author: Hisataka Kobayashi, M.D., Ph.D. Molecular Imaging Program, Center for Cancer Research, National Cancer Institute, NIH, Building 10, Room 1B40, MSC1088, Bethesda, MD 20892-1088. Phone: 301-451-4220; Fax: 301-402-3191; kobayash@mail.nih.gov.

utilized for molecular imaging, including nuclear imaging, optical imaging, MRI and ultrasound (1-3). Based on the physical characteristics of the emitted signals and the signal detection systems, each modality has both advantages and disadvantages. As a result, multimodality imaging should have the potential for overcoming the disadvantages of a single modality by combining the advantages of more than one modality.

Both nuclear imaging and optical imaging have comparable high sensitivities, however, nuclear imaging is superior for quantification due to good tissue penetration of gamma rays and the ability to accurately measure count rate in tissue, which permits whole body quantitative imaging not only in small animals but also in humans. However, it is impossible to control or "switch off" ionizing radiation *in vivo* because there are no bioavailable materials to quench gamma rays. Therefore, target specificity can be compromised by the high background signals originating from unbound or nonspecifically bound probes due to the "always on" feature of nuclear imaging probes, especially when slow clearing probes including monoclonal antibodies are employed (4,5).

In contrast, optical imaging can be superior to nuclear imaging for target-specificity because it can employ target-specific activatable systems. In these activatable systems, the fluorescent signal can be quenched by one of several mechanisms, and the quenched signal can subsequently be turned on in particular biological environments such as lowered pH. We and other groups have developed a number of target-specific activatable optical probes using several mechanisms, e.g. FRET-quenching, pH activation, self-quenching and H-dimer formation (6-13). The fluorescent signals of these activatable probes are designed to be switched on only in the target cells or tissues. As a result, the background and non-specific signal is dramatically reduced. However, optical imaging techniques are not quantitative, especially when the object is located deep to the skin because of significant signal attenuation in tissue. Near-infrared (NIR, emission spectra ~700-850 nm) fluorescence is one of the potential solutions for overcoming this limitation, although the penetration of NIR is still lower than gamma rays (14-16). Among the NIR dyes, indocyanine green (ICG) is a fluorescence dye that has long been approved by the FDA for clinical use in retinal angiography and for intraoperative assessment of liver function (17,18). However, ICG-conjugated antibodies were considered not useful for molecular imaging, because all ICG-conjugated antibodies examined in the literature yielded faint fluorescent signals and were not successful even in *in vitro* assays (19,20). Recently, we demonstrated that ICG-conjugated monoclonal antibodies are able to target cells expressing the receptor, during *in vivo* molecular imaging (21). The fluorescent signal of an ICG-conjugated monoclonal antibody is quenched when the probe is unbound or located outside of the target cell, however, it activates, when the probe is bound and internalized into the target cells. Therefore, an ICG-conjugated antibody can specifically visualize the target tumor with minimal background signal.

In this study, multimodality imaging was performed by the use of a radiolabeled antibody and a target cell-specific activatable NIR fluorescence-labeled antibody. We employed FDA approved monoclonal antibodies, panitumumab (anti-HER1) and trastuzumab (anti-HER2) as internalizing targeting ligands. These antibodies were labeled with ^{111}In and ICG for radio-optical imaging, and tested in both HER1 and HER2 tumor bearing mice using an injection of a cocktail of radiolabeled and optical antibodies, and by the single injection of a dual-labeled antibody.

MATERIALS AND METHODS

Reagents

Panitumumab, a human anti-HER1 antibody, was purchased from AMGEN Inc. (Thousand Oaks, CA). Trastuzumab, a humanized anti-HER-2 antibody, was purchased from Genentech

Inc. (South San Francisco, CA). ICG-sulfo-OSu was purchased from Dojindo Molecular Technologies (Rockville, MD). 2-(4-Isothiocyanatobenzyl)-diethylenetriamine pentaacetic acid (*p*-SCN-BzDTPA) was purchased from Macrocyclics (Dallas, TX). Carrier-free $^{111}InCl_3$ was purchased from Perkin-Elmer Health Sciences, Inc. (North Billerica, MA). All other chemicals used were of reagent grade.

Cell culture

The HER1 positive cell lines, A431 and MDA-MB468 were used for HER1 targeting studies with panitumumab conjugates. For HER2 targeting studies by trastuzumab conjugates, the *HER2* gene transfected NIH3T3 (3T3/HER2) cell line was used. The cell lines were grown in RPMI 1640 (Life Technologies, Gaithersburg, MD) containing 10% fetal bovine serum (Life Technologies), 0.03% L-glutamine, 100 units/mL penicillin, and 100 μg/mL streptomycin in 5% CO_2 at 37°C.

Synthesis of ICG conjugated antibodies

Panitumumab or trastuzumab (1 mg, 6.8 nmol) was incubated with ICG-sulfo-OSu (68 nmol) in 0.1M Na_2HPO_4 (pH 8.5) at room temperature for 30 min. Then, the mixture was purified with a Sephadex™ G50 column (PD-10; GE Healthcare, Piscataway, NJ). The concentration of ICG was measured by absorption with the UV-Vis system to confirm the number of fluorophore molecules conjugated to each antibody molecule under conditions of 5% SDS and 2-mercapto ethanol (2-ME) which diminish intermolecular interaction among ICG molecules and between ICG and the antibody. The number of ICG per antibody was ~4-5.

Radiolabeling of antibodies

Panitumumab or trastuzumab was reacted with 15-fold molecular excess of *p*-SCN-Bn-DTPA at pH 8.5 in sodium hydrogen carbonate buffer for 1 hr at 25°C. The Bn-DTPA conjugated antibodies were purified by dialysis using 1xPBS on an Amicon® Ultra-4 centrifugal device with Ultracel-30 (Millipore, Danvers, MA). Indium-111 chloride (3.5 μL of 295 MBq stock in 0.05M HCl) is added to the Bn-DTPA a ntibody conjugate (100 μg) in 25 μL 0.15 M NH 4OAc pH ~7 and incubated for 1 hr at room temperature. EDTA (5 μL of 0.1 M) was then added to quench the react ion mixture. The radiolabeled antibody was then purified using a Sephadex™ G-25 column (PD 10; GE Healthcare) eluted with 1xPBS. The radiolabeled antibody fraction was collected and the specific activities of the radiolabeled antibodies were 211 and 210 MBq/mg for ^{111}In-panitumumab and ^{111}In-trastuzumab, respectively. Radiochemical purities were assessed by radio-ITLC and were 81% and 88% for the ^{111}In-panitumumab and ^{111}In-trastuzumab, respectively.

Dual-labeling of antibody with ICG and ^{111} In

Trastuzumab (1 mg, 6.8 nmol) was incubated with ICG-sulfo-OSu (13.6 nmol) in 0.1M Na_2HPO_4 (pH 8.5) at room temperature for 30 min. Then, the mixture was purified as described above. The number of ICG per antibody was ~1. Trastuzumab-ICG was then treated with 15-fold molecular excess of *p*-SCN-BzDTPA. The resulted ICG and BzDTPA conjugated trastuzumab was labeled with ^{111}In and purified in the same manner as above. The specific activity was 404 MBq/mg and the radiochemical purity was 89 %.

Immunoreactivity of radiolabeled conjugates

Immunoreactivity of ^{111}In-panitumumab, ^{111}In-trastuzumab or ^{111}In-trastuzumab-ICG was determined using a previously described method in cultured cell lines (22,23). In brief, aliquots of the radiolabeled antibodies (2.6 ng) were incubated for 1 hr at 4°C with 2×10^6 A431 or 3T3/HER2 for panitumumab or trastuzumab conjugates, respectively. The cell binding fraction was collected by centrifuge, and the radioactivity of the cell and supernatant fractions were

counted in a gamma-counter. Non-specific binding to the cells was determined by adding excess unlabeled antibody.

Investigation of fluorescence characteristics of ICG conjugated antibodies *in vitro*

The fluorescence characteristics of ICG conjugated antibodies were investigated by treating the conjugates with 5% SDS and 2-ME to diminish the hydrophobic interactions and separate the IgG chains. The change in fluorescence intensity for each conjugate was investigated with an *in vivo* imaging system (Maestro™, CRi Inc., Woburn, MA) using 710 to 760 nm excitation and 800 nm long-pass emission filters.

Fluorescence microscopy studies

3T3/HER2 or A431 cells were plated on a cover glass-bottomed culture well and incubated for 16 h. Then, trastuzumab-ICG or panitumumab-ICG was added to the medium (10 μg/mL), and the cells were incubated for either 1 or 8 hrs. Cells were washed once with PBS, and fluorescence microscopy was performed using an Olympus BX61 microscope (Olympus America, Inc., Melville, NY) equipped with the following filters: excitation wavelength 672.5 to 747.5 nm, emission wavelength 765 to 855 nm. Transmitted light differential interference contrast images were also acquired.

Animal Tumor Model

All procedures were carried out in compliance with the Guide for the Care and Use of Laboratory Animal Resources (1996), National Research Council, and approved by the local Animal Care and Use Committee. A431 cells (HER1+, HER2−, 2×10^6 cells) were injected subcutaneously in the left dorsum of the female nude mice (National Cancer Institute Animal Production Facility, Frederick, MD), and 3T3/HER2 cells (HER1−, HER2+, 2×10^6 cells) were injected subcutaneously into the right dorsum. The experiments were performed at 10 - 17 days after cell injection. For dual labeled antibody studies by ^{111}In-trastuzumab-ICG, the following cells, MDA-MB468 (HER1+, HER2−, 2×10^6 cells), A431 (HER1+, HER2−, 2×10^6 cells) and 3T3/HER2 (HER1−, HER2+, 2×10^6 cells), were injected subcutaneously into the left flank, right buttock and right flank, respectively.

In vivo multimodal imaging studies by fluorescent and radioactive antibodies

A cocktail of panitumumab-ICG (50 μg) and ^{111}In-panitumumab (4.2 MBq/10 μg) or trastuzumab-ICG (50 μg) and ^{111}In-trastuzumab (4.2 MBq/10 μg) was injected intravenously into A431 and 3T3/HER2 tumor bearing mice (n = 4, each). The optical and nuclear images were obtained by Maestro™ (CRi Inc., Woburn, MA) and an in-house built flat panel gamma gamera (Mobile Nuclear Imaging Camera, MONICA) imaging system, respectively, over 6 days after the injection.

For fluorescence imaging, a 710-760 nm band-pass filter was used for excitation and a long-pass filter over 700 nm was used for emission. The spectral fluorescence images consisting of autofluorescence spectra and the spectra from ICG were then unmixed based on their spectral patterns using commercial software (Maestro software, CRi, Inc., Woburn, MA). The regions of interest were placed on the ICG spectral images to measure the fluorescence intensities of the A431 and 3T3/HER2 tumors.

The scintigram of each mouse was obtained by 5min scan with MONICA, (see above) (24). Then, the images were processed using Image-J software (National Institutes of Health, Bethesda, MD, http://rsb.info.nih.gov/ij/). The regions of interest were placed on the scintigram, and the accumulated radioactivity was measured.

After the imaging on day 6, the mice were sacrificed with carbon dioxide and *ex vivo* images of the resected organs were obtained with both modalities as with the *in vivo* imaging. Then, the organs were weighed and counted in a gamma counter to calculate %ID/g. For histological validation, the dissected lesions were embedded in paraffin and stained with Hematoxylin and Eosin (H&E).

In vivo multimodal imaging studies with dual labeled antibodies

To investigate the effect of pharmacokinetic properties on imaging by radio-optical labeled antibodies, ^{111}In-trastuzumab-ICG (3.8 MBq/60 μg) was injected intravenously into the 3-tumor bearing mice (A431 (HER1+), MDA-MB468 (HER1+), 3T3/HER2 (HER2+)). The optical and nuclear images were obtained over time and processed in the same manner as above.

RESULTS

Immunoreactivity of radiolabeled antibodies

The immumoreactivity of the ^{111}In-panitumumab and ^{111}In-trastuzumab were 64% and 69%, respectively. The immunoreactivity of the dual-labeled probe, ^{111}In-trastuzumab-ICG was 75%.

The fluorescence quenching of ICG conjugated antibodies

The fluorescence quenching capacity was measured by treating the conjugates with SDS and 2-ME to dissociate the interactions between ICG molecules, and between ICG and its antibody. The fluorescence intensity was very low before the SDS and 2-ME treatment (Figure 1). Intense fluorescence was detected after dissociation and the quenching capacities were calculated at 17.4, 19.1 and 7.3 fold, for panitumumab-ICG, trastuzumab-ICG and BzDTPA-trastuzumab-ICG, respectively.

In vitro fluorescence microscopic studies

To investigate the fluorescence activation in the target cells, microscopy was performed. The results are summarized in Figure 2. Fluorescence was not observed for either panitumumab-ICG or trastuzumab-ICG after 0.5 hr incubation, when the conjugates were still outside the cells and bound to cell surface receptors. After the conjugates were internalized into the cells after 8 hr incubation, both conjugates showed bright fluorescence signal within the target cells. These results demonstrate that both panitumumab-ICG and trastuzumab-ICG are capable of activation, that is, the signal is switched on only within target cancer cells.

In vivo multimodality imaging studies

The results of the cocktail injection of radio- and fluorescently-labeled probes are summarized in Figure 3 and Figure 4. With ^{111}In-panitumumab, radioactivity gradually accumulated in the target tumor (A431, HER1+), while the non-target tumor (3T3/HER2) was not detected. ^{111}In-Trastuzumab showed both target specific (3T3/HER2) and non-specific (A431, HER1+) tumors. A high liver signal was observed in both antibodies. The biodistribution results were consistent with gamma scintigraphy (Figure 5). In contrast, fluorescent signal from both antibodies was activated beginning one day after the injection, although the background signal was detected just after the conjugate injections. Images of the dissected organs by both modalities confirmed these observations. That is, only the target specific tumors were visualized with optical imaging, while, the biodistribution profile of the injected antibodies were provided by nuclear imaging.

To confirm that pharmacokinetic properties did not affect the results above, radio-optical dual labeled trastuzumab was injected in mice bearing 3 tumors. The nuclear images showed A431

(HER1+) and liver uptake as well as 3T3/HER2 tumor uptake. MDA-MB468 (HER1+) tumor was not detected (Figure 3C). In contrast, fluorescent imaging only detected 3T3/HER2 tumor.

The H&E staining showed that the A431 tumor (HER1) had greater vascular density than 3T3/HER2 (HER2) tumor (Figure 3D).

DISCUSSION

Multimodality molecular imaging can provide molecular information *in vivo* using two more imaging technologies. Some investigators have already reported radio-optical labeling of probes and have succeeded in yielding nearly identical signals from both modalities despite differences in the physical characteristics of radiation and fluorescence signals (25-30). These imaging results reflect the biodistribution of the labeled probe because researchers generally have used “always on” optical probes, which yield signals similar to radionuclides. However, by acquiring different signals *i.e.* “always on” and target-specific activatable probes (“conditionally on”), additional information could be obtained.

In this study, we showed that activatable fluorescence imaging was capable of cell specific signal activation and thus highly specific imaging, while radioactive antibodies were more quantitative. The humanized antibodies, panitumumab (anti-HER1) and trastuzumab (anti-HER2) were selected as targeting moieties for molecular imaging in this study, because cancer-specific antigens are attractive “theragnostic” targets, and antibodies for these antigens are promising for seeing and treating cancers. Specific visualization of the target molecule is an important goal for accurate cancer characterization. At the same time, it is also important to visualize the delivery of targeted therapeutic molecules quantitatively for the effective treatment.

As expected, ICG-conjugated antibodies functioned as activatable optical probes emitting in the NIR and the baseline (non-internalized) fluorescence signal was vanishingly low *in vitro* (Figure 1). This was confirmed with microscopy of cultured cells as shown in Figure 2. When the probe is binding to the cell surface antigen (1hr of incubation), no fluorescence signal could be detected, however, when the conjugate was internalized (8hrs of incubation), fluorescent signal was easily detectable. If the always-on fluorescent probe was used for this investigation, the surface fluorescent signal can be clearly detected by 1hr incubation (Supplemental figure 1). Although the mechanism is still under investigation, we suggest that the strong negative charge due to the ICG's sulfonate groups might facilitate the interaction between the ICG and basic amino acid sequences on the IgG cause loss of fluorescence from ICG. By combination with the classic self-quenching system, ICG conjugated antibody might be able to produce high quenching capacities. In fact, the other NIR dye, cypate, which has a similar chemical structure to ICG with carboxylic acid groups instead of sulfonate groups, can label the peptides without the fluorescence quenching (31,32).

Since sulfonate is a stronger acid than carboxylate, the negative charge effect should be weaker for cypate than ICG. Unlike to other near infrared dyes with carboxyl substitutes for sulfonate groups, free ICG is strongly incorporated with albumin probably the similar reason. The lipophilicity might be another cause for fluorescence quenching by the hydrophobic interaction between dye molecule and hydrophobic amino acid sequences. However, DMSO did not affect the fluorescence de-quenching of the ICG conjugated antibody (Supplemental figure 2) that suggests the minimal contribution of the hydrophobicity.

This unique feature of this ICG-conjugated antibody contributed to achieve fluorescence imaging with minimal background signal, when bound to the target and internalized into the living cells. In contrast, other researchers reported a few limited successes in the literatures. Only a weak fluorescence was observed, when ICG-conjugated antibodies were applied for *in*

vitro assays using sliced tissue samples, although the fluorescence yield of the ICG-conjugates were slightly improved by changing the chemical linkage (20). Withrow et al. applied an ICG-conjugated antibody (cetuximab, anti-EGFR antibody) for imaging xenografted tumors in mice, however, they concluded that the sensitivity of this probe for cancer detection was low. This might be due to the smaller target numbers on the tumor cells or less efficient internalization process of the ICG-antibody conjugates than the cells, which we used in this study. Although their ICG-conjugated antibody appeared to be brighter than our quenched conjugate, 7-fold larger amount of the ICG-conjugated antibody (350 μg) was injected t o the mice, therefore, they might detect fluorescence signal not only from tumor but also from the background normal tissues because large amount of unbound probes remaining in the body could yield the fluorescence signal (33).

Then, we tested our multimodality imaging strategy by injecting radio-optically labeled antibody cocktails into the HER1+ and HER2+ tumor bearing mice. As expected, only the target specific tumor was visualized by optical imaging (Figure 3, 4). The observed background signal just after the ICG-conjugated antibodies injection might be due to the physiological excretion of non-covalently bound or catabolized ICG, which was dissociated from the antibody immediately after the injection and complexed with albumin. The ICG-albumin complex is highly fluorescent but it is rapidly eliminated from the body of normal subjects through the liver (34).

In contrast, radioactive signal could be detected from whole body (blood pool), the liver and the spleen as well as the target tumor. The non-target tumor was also imaged in HER2 targeting studies. Since the vascularity of A431 tumor (HER1) was higher than 3T3/HER2 (HER2+) tumor (Figure 3D), the reason for the visualization of A431 tumor with ^{111}In-trastuzumab is thought to be due to its high blood supply and enhanced permeability and retention (EPR) effect (35, 36). As indicated in Figure5, a certain level of radioactivity remained in the blood especially for ^{111}In-trastuzumab even 6 days after the injection. The EPR effect depends only on the physical characteristics of the macromolecules injected and not on their binding characteristics and thus, it often leads to non-specific tumor uptake.

Thus, target specific images were successfully obtained with activatable optical probes, while quantitative antibody biodistribution was provided by the “always on” radioactive probes. The difference between optical and nuclear imaging was not caused by differences in their pharmacokinetic properties, because the same results were obtained with the dual-labeled antibody (Figure 3C).

A limitation of optical imaging is difficulty in deep tissue detection. NIR fluorescence is one solution for this problem because of the better tissue penetration of NIR light in tissue (14). Recently, diffuse optical tomography has improved the deep tissue sensitivity (37). This technique can visualize the target at ~50mm depth volumetrically using NIR probes, and it might be applicable for human breast cancer imaging as well as small animal imaging. At the same time, optical imaging can make a significant contribution when it is utilized during endoscopy or surgery, because activatable optical probes can achieve fairly low background signals (7,8). Thus, whole body imaging with radionuclides followed by optically guided surgery is a promising direction for multimodality imaging. Furthermore, optical imaging has the potential to add more functional information, for example, by using multicolor imaging or fluorescence lifetime imaging (38-42).

In conclusion, we characterized molecular targets with activatable optical probes, and visualized and quantified the delivery of targeted antibodies using radioactive labeling. Recently, the Molecular Imaging Center of Excellence stated that “Molecular imaging is the visualization, characterization, and measurement of biological processes at the molecular and

cellular levels in humans and other living systems" (43). Multimodality molecular imaging, by combining activatable optical probes with radioactive probes, has great potential for achieving this definition.

Supplementary Material

Refer to Web version on PubMed Central for supplementary material.

Acknowledgments

This research was supported by the Intramural Research Program of the NIH, National Cancer Institute, Center for Cancer Research.

References

1. Frangioni JV. New technologies for human cancer imaging. J Clin Oncol 2008;26:4012–4021. [PubMed: 18711192]
2. Hoffman JM, Gambhir SS. Molecular imaging: the vision and opportunity for radiology in the future. Radiology 2007;244:39–47. [PubMed: 17507723]
3. Weissleder R, Pittet MJ. Imaging in the era of molecular oncology. Nature 2008;452:580–589. [PubMed: 18385732]
4. Wu AM. Antibodies and antimatter: the resurgence of immuno-PET. J Nucl Med 2009;50:2–5. [PubMed: 19091888]
5. Wu AM, Senter PD. Arming antibodies: prospects and challenges for immunoconjugates. Nat Biotechnol 2005;23:1137–1146. [PubMed: 16151407]
6. Bremer C, Tung CH, Weissleder R. In vivo molecular target assessment of matrix metalloproteinase inhibition. Nat Med 2001;7:743–748. [PubMed: 11385514]
7. Hama Y, Urano Y, Koyama Y, Gunn AJ, Choyke PL, Kobayashi H. A self-quenched galactosamine-serum albumin-rhodamineX conjugate: a "smart" fluorescent molecular imaging probe synthesized with clinically applicable material for detecting peritoneal ovarian cancer metastases. Clin Cancer Res 2007;13:6335–6343. [PubMed: 17975145]
8. Hama Y, Urano Y, Koyama Y, Kamiya M, Bernardo M, Paik RS, Shin IS, Paik CH, Choyke PL, Kobayashi H. A target cell-specific activatable fluorescence probe for in vivo molecular imaging of cancer based on a self-quenched avidin-rhodamine conjugate. Cancer Res 2007;67:2791–2799. [PubMed: 17363601]
9. Kamiya M, Kobayashi H, Hama Y, Koyama Y, Bernardo M, Nagano T, Choyke PL, Urano Y. An enzymatically activated fluorescence probe for targeted tumor imaging. J Am Chem Soc 2007;129:3918–3929. [PubMed: 17352471]
10. Mahmood U, Tung CH, Bogdanov A Jr. Weissleder R. Near-infrared optical imaging of protease activity for tumor detection. Radiology 1999;213:866–870. [PubMed: 10580968]
11. Ogawa M, Kosaka N, Longmire MR, Urano Y, Choyke PL, Kobayashi H. Fluorophore-Quencher Based Activatable Targeted Optical Probes for Detecting in Vivo Cancer Metastases. Mol Pharm 2009;6:386–395. [PubMed: 19718793]
12. Ogawa M, Regino CA, Choyke PL, Kobayashi H. In vivo target-specific activatable near-infrared optical labeling of humanized monoclonal antibodies. Mol Cancer Ther 2009;8:232–239. [PubMed: 19139133]
13. Urano Y, Asanuma D, Hama Y, Koyama Y, Barrett T, Kamiya M, Nagano T, Watanabe T, Hasegawa A, Choyke PL, Kobayashi H. Selective molecular imaging of viable cancer cells with pH-activatable fluorescence probes. Nat Med 2009;15:104–109. [PubMed: 19029979]
14. Frangioni JV. In vivo near-infrared fluorescence imaging. Curr Opin Chem Biol 2003;7:626–634. [PubMed: 14580568]
15. Sharma R, Wendt JA, Rasmussen JC, Adams KE, Marshall MV, Sevick-Muraca EM. New horizons for imaging lymphatic function. Ann N Y Acad Sci 2008;1131:13–36. [PubMed: 18519956]

16. Weissleder R. A clearer vision for in vivo imaging. Nat Biotechnol 2001;19:316–317. [PubMed: 11283581]
17. Dzurinko VL, Gurwood AS, Price JR. Intravenous and indocyanine green angiography. Optometry 2004;75:743–755. [PubMed: 15624671]
18. Sakka SG. Assessing liver function. Curr Opin Crit Care 2007;13:207–14. [PubMed: 17327744]
19. Muguruma N, Ito S, Hayashi S, Taoka S, Kakehashi H, Ii K, Shibamura S, Takesako K. Antibodies labeled with fluorescence-agent excitable by infrared rays. J Gastroenterol 1998;33:467–471. [PubMed: 9719226]
20. Tadatsu M, Ito S, Muguruma N, Kusaka Y, Inayama K, Bando T, Tadatsu Y, Okamoto K, Ii K, Nagao Y, Sano S, Taue H. A new infrared fluorescent-labeling agent and labeled antibody for diagnosing microcancers. Bioorg Med Chem 2003;11:3289–3294. [PubMed: 12837539]
21. Ogawa M, Kosaka N, Choyke PL, Kobayashi H. In vivo molecular imaging of cancer with a quenching near-infrared fluorescent probe using conjugates of monoclonal antibodies and indocyanine green. Cancer Res 2009;69:1268–1272. [PubMed: 19176373]
22. Barrett T, Koyama Y, Hama Y, Ravizzini G, Shin IS, Jang BS, Paik CH, Urano Y, Choyke PL, Kobayashi H. In vivo diagnosis of epidermal growth factor receptor expression using molecular imaging with a cocktail of optically labeled monoclonal antibodies. Clin Cancer Res 2007;13:6639–6648. [PubMed: 17982120]
23. Kobayashi H, Yoo TM, Kim IS, Kim MK, Le N, Webber KO, Pastan I, Paik CH, Eckelman WC, Carrasquillo JA. L-lysine effectively blocks renal uptake of 125I- or 99mTc-labeled anti-Tac disulfide-stabilized Fv fragment. Cancer Res 1996;56:3788–3795. [PubMed: 8706025]
24. Xi W, Seidel J, Kakareka J, Proffitt J, Pohida T, Majewski S, Weisenberger AG, Green MV, Choyke PL. 2008 World Molecular Imaging Congress abstract book 2008:#0412.
25. Cai W, Chen K, Li ZB, Gambhir SS, Chen X. Dual-function probe for PET and near-infrared fluorescence imaging of tumor vasculature. J Nucl Med 2007;48:1862–1870. [PubMed: 17942800]
26. Culver J, Akers W, Achilefu S. Multimodality molecular imaging with combined optical and SPECT/PET modalities. J Nucl Med 2008;49:169–172. [PubMed: 18199608]
27. Houston JP, Ke S, Wang W, Li C, Sevick-Muraca EM. Quality analysis of in vivo near-infrared fluorescence and conventional gamma images acquired using a dual-labeled tumor-targeting probe. J Biomed Opt 2005;10:054010. [PubMed: 16292970]
28. Li C, Wang W, Wu Q, Ke S, Houston J, Sevick-Muraca E, Dong L, Chow D, Charnsangavej C, Gelovani JG. Dual optical and nuclear imaging in human melanoma xenografts using a single targeted imaging probe. Nucl Med Biol 2006;33:349–358. [PubMed: 16631083]
29. Sampath L, Kwon S, Ke S, Wang W, Schiff R, Mawad ME, Sevick-Muraca EM. Dual-labeled trastuzumab-based imaging agent for the detection of human epidermal growth factor receptor 2 overexpression in breast cancer. J Nucl Med 2007;48:1501–1510. [PubMed: 17785729]
30. Vera DR, Hall DJ, Hoh CK, Gallant P, McIntosh LM, Mattrey RF. Cy5.5-DTPA-galactosyl-dextran: a fluorescent probe for in vivo measurement of receptor biochemistry. Nucl Med Biol 2005;32:687–693. [PubMed: 16243643]
31. Achilefu S, Bloch S, Markiewicz MA, Zhong T, Ye Y, Dorshow RB, Chance B, Liang K. Synergistic effects of light-emitting probes and peptides for targeting and monitoring integrin expression. Proc Natl Acad Sci U S A 2005;102:7976–7981. [PubMed: 15911748]
32. Bloch S, Xu B, Ye Y, Liang K, Nikiforovich GV, Achilefu S. Targeting Beta-3 integrin using a linear hexapeptide labeled with a near-infrared fluorescent molecular probe. Mol Pharm 2006;3:539–549. [PubMed: 17009853]
33. Withrow KP, Gleysteen JP, Safavy A, Skipper J, Desmond RA, Zinn K, Rosenthal EL. Assessment of indocyanine green-labeled cetuximab to detect xenografted head and neck cancer cell lines. Otolaryngol Head Neck Surg 2007;137:729–734. [PubMed: 17967636]
34. Faybik P, Hetz H. Plasma disappearance rate of indocyanine green in liver dysfunction. Transplant Proc 2006;38:801–802. [PubMed: 16647475]
35. Baban DF, Seymour LW. Control of tumour vascular permeability. Adv Drug Deliv Rev 1998;34:109–119. [PubMed: 10837673]
36. Torchilin VP. Drug targeting. Eur J Pharm Sci 2000;11(Suppl 2):S81–91. [PubMed: 11033430]

37. Ntziachristos V, Ripoll J, Wang LV, Weissleder R. Looking and listening to light: the evolution of whole-body photonic imaging. Nat Biotechnol 2005;23:313–320. [PubMed: 15765087]

38. Hosokawa R, Kambara N, Ohba M, Mukai T, Ogawa M, Motomura H, Kume N, Saji H, Kita T, Nohara R. A catheter-based intravascular radiation detector of vulnerable plaques. J Nucl Med 2006;47:863–867. [PubMed: 16644757]

39. Kobayashi H, Hama Y, Koyama Y, Barrett T, Regino CA, Urano Y, Choyke PL. Simultaneous multicolor imaging of five different lymphatic basins using quantum dots. Nano Lett 2007;7:1711–1716. [PubMed: 17530812]

40. Kobayashi H, Koyama Y, Barrett T, Hama Y, Regino CA, Shin IS, Jang BS, Le N, Paik CH, Choyke PL, Urano Y. Multimodal nanoprobes for radionuclide and five-color near-infrared optical lymphatic imaging. ACS Nano 2007;1:258–264. [PubMed: 19079788]

41. Kosaka N, Ogawa M, Longmire MR, Choyke PL, Kobayashi H. Multi-targeted multi-color in vivo optical imaging in a model of disseminated peritoneal ovarian cancer. J Biomed Opt 2009;14:014023. [PubMed: 19256711]

42. Longmire M, Kosaka N, Ogawa M, Choyke PL, Kobayashi H. Multicolor in vivo targeted imaging to guide real-time surgery of HER2-positive micrometastases in a two-tumor coincident model of ovarian cancer. Cancer Sci 2009;100:1099–1104. [PubMed: 19302283]

43. Mankoff DA. A definition of molecular imaging. J Nucl Med 2007;48:18N, 21N.

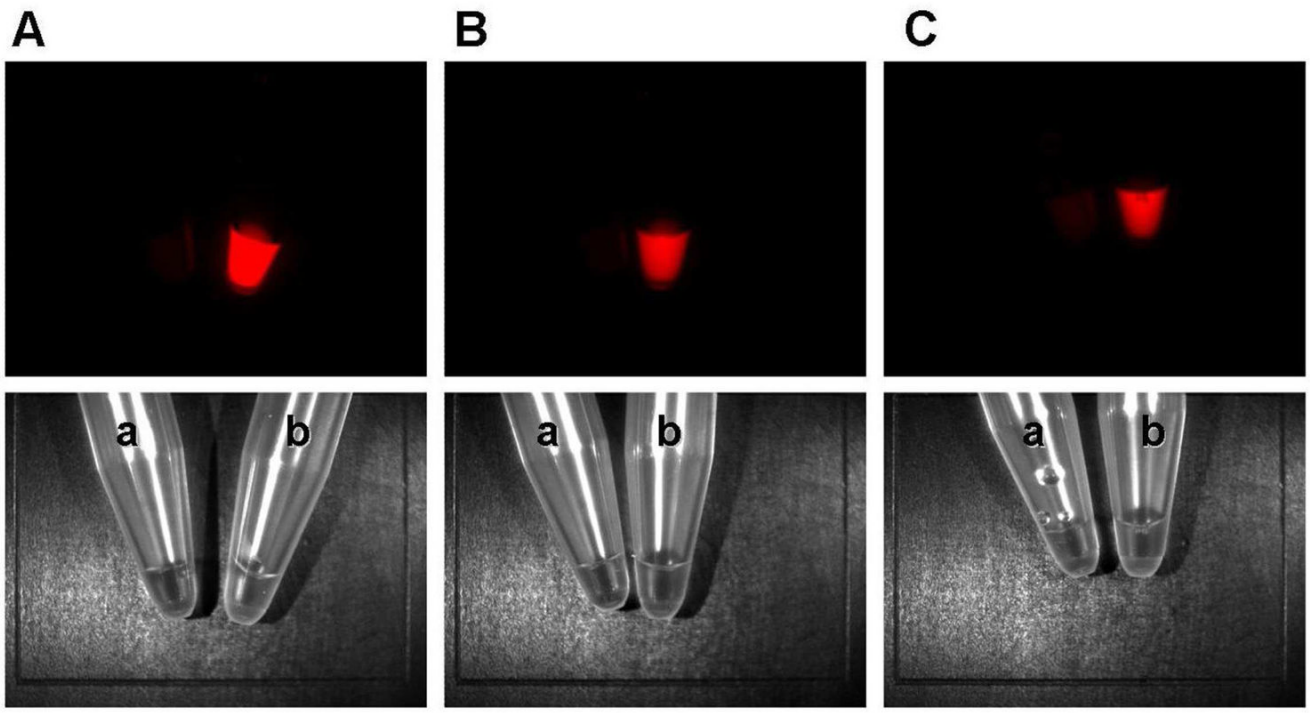

Figure 1.
The fluorescence and white light images of antibody-ICG conjugates. a: panitumumab-ICG, b: trastuzumab-ICG, c: BzDTPA-trastuzumab-ICG. A: in PBS, B: SDS and 2-ME added condition. In PBS, the conjugates have no fluorescence. Fluorescence is activated by SDS and 2-ME treatment.

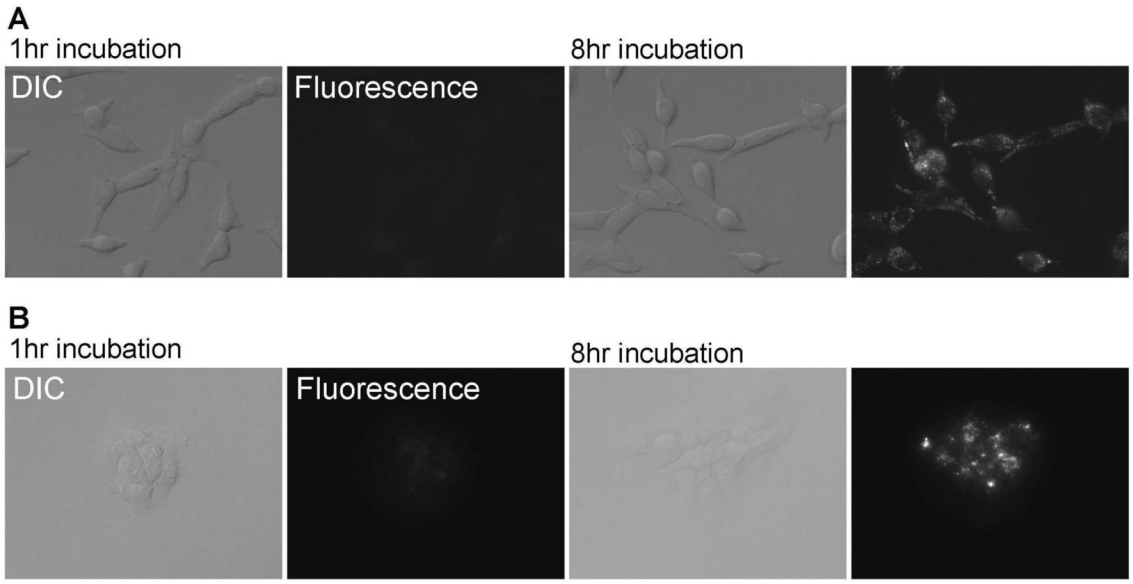

Figure 2.
Fluorescence microscopy and differential interference contrast (DIC) images. A431 cells were incubated with panitumumab-ICG (a) and 3T3/HER2 cells were incubated with trastuzumab-ICG (b) for either 1hr or 8hrs. The fluorescent signal was detected after internalization into the cells by 8hr incubation.

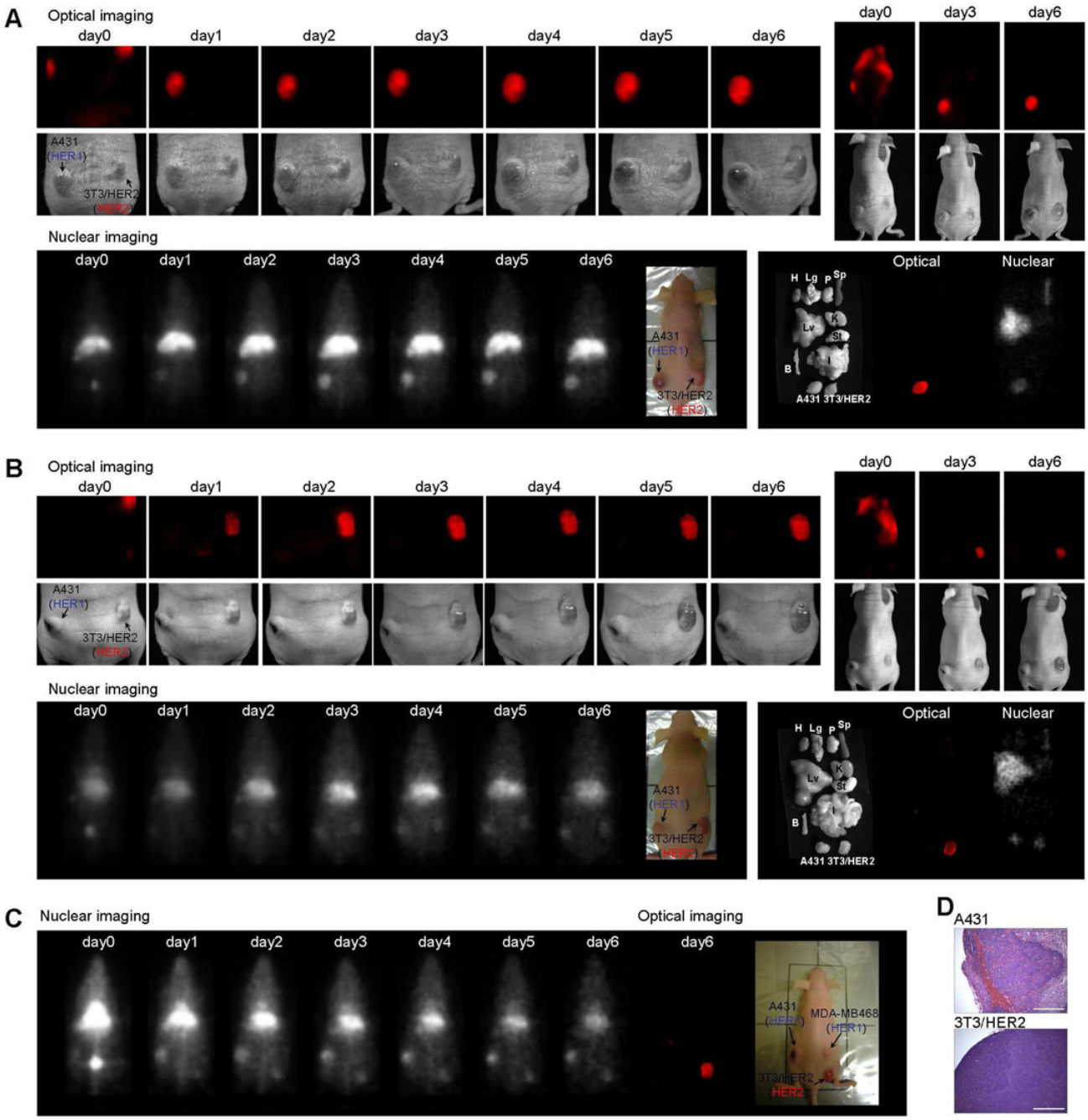

Figure 3.

Multimodality imaging results after a cocktail injection of panitumumab-ICG and 111Inpanitumumab (a) or trastuzumab-ICG and 111In-trastuzumab (b), and the results with dual-labeled probe, 111In-trastuzumab-ICG (c). Only the target tumor was visualized by optical imaging, in contrast, antibody distribution could be determined by nuclear imaging. d: HE staining of dissected tumors. The vascularity was higher in A431 tumor than 3T3/HER2 tumor. H; Heart, Lg; Lung, P; Pancreas, Sp; Spleen, Lv; Liver, K; Kidney, St; Stomach, B; Bone, I; Intestine

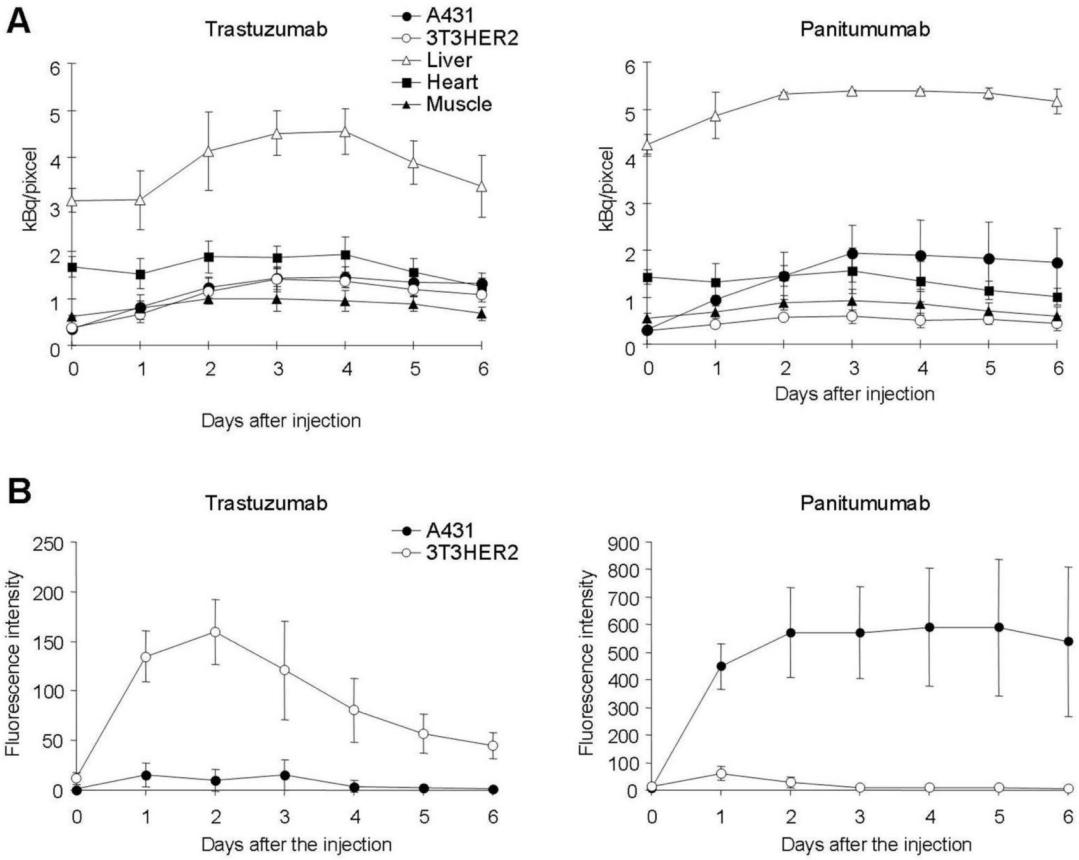

Figure 4.

Time course of radioactivity (a) and fluorescence (b) intensities after the injection of a cocktail of panitumumab-ICG and 111In-panitumumab or trastuzumab-ICG and 111In-trastuzumab. High liver uptake was observed on radionuclide scans. The fluorescent signals were increased only in the target tumors, but the signal intensities of target and non-target tumor were identical in 111Intrastuzumab treated mice.

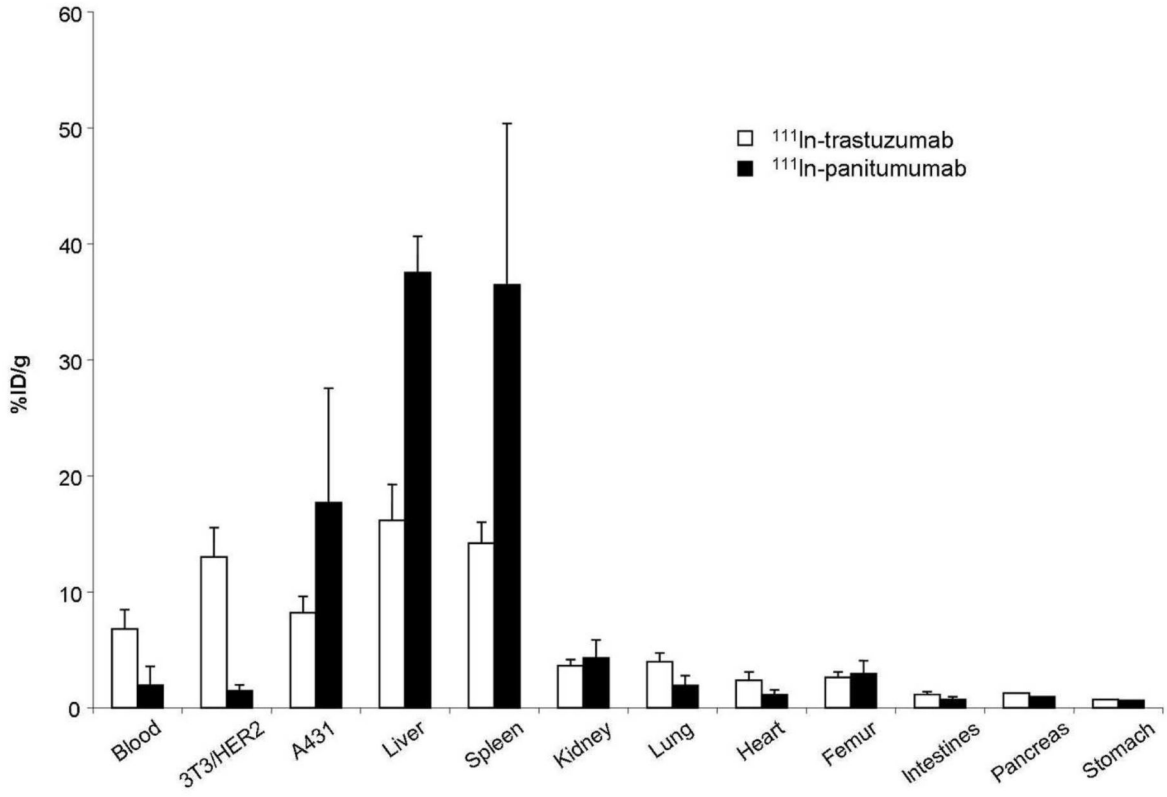

Figure 5.

Biodistribution of 111In-panitumumab and 111In-trastuzumab immediately after obtaining 6 day images was shown. The biodistribution results were consistent with images obtained 6 day after injection taken with the MONICA dual camera system.